Application of the Virtual Fields Method to fracture mechanics

M. Rossi, M. Fardmoshiri, M. Sasso, D. Amodio
DIISM, Università Politecnica delle Martche, Ancona (Italy)
m.rossi@univpm.it

ABSTRACT. The Virtual Fields Method (VFM) is an inverse method which allows to identify the mechanical properties of material starting from full-field measurements. Thanks to its adaptability it has been applied to several fields of mechanical engineering as, for instance, the identification of the stiffness of composites, the vibration analysis and, recently, the elasto-plasticity. The aim of this paper is using the VFM and full-field measurements to identify the plastic zone close to the crack tip. The potentiality and the limits of the method are investigated with simulated experiments which reproduce the measurement of the deformation fields close to the crack in a standard CT-test. Different spatial resolutions and noise levels were taken into account.

SOMMARIO. Il Virtual Fields Method (metodo dei campi virtuali, VFM) è un metodo inverso che consente di identificare le proprietà dei materiali a partire da misure di campo di deformazione. Grazie alla sua flessibilità è stato applicato in numerosi campi dell'ingegneria meccanica, come ad esempio nella determinazione della rigidezza di compositi, nell'analisi di vibrazioni e, recentemente, nello studio della plasticità. In questo lavoro ci si propone di utilizzare il VFM per determinare la zona plastica all'apice di una cricca a partire da misure di campo di deformazione. Le potenzialità e i limiti del metodo sono studiate tramite esperimenti simulati che riproducono l'acquisizione del campo di deformazione all'apice di un difetto in un CT-test standard. Diverse risoluzioni spaziali e livelli di rumorosità della misura sono trattati.

KEYWORDS. Plastic radius; Virtual Fields Method; CT test; Elasto-plastic fatigue.

INTRODUCTION

The Virtual Fields Method (VFM) allows identifying the mechanical properties of materials from full-field displacement and strain measurements [1]. Such a method was originally developed to identify the stiffness parameters of orthotropic materials, however, thanks to its adaptability, it was subsequently extended to many other different fields, e.g. plasticity [2,3], hyper-elasticity [4,5], dynamic testing [6], vibration [7], etc. The VFM relies on the principle of virtual work and is applied to experimental tests which produce heterogeneous strain fields. It has several advantages compared to other inverse methods, as, for instance, the finite element updating method [8]. For instance, the VFM can easily deal with complex boundary conditions, specimen misalignments or not perfect specimen shapes, and the computational time is low, since no FE simulations are required. On the other hand, the results are strongly influenced by the accuracy of the strain measurements and, accordingly, by the adopted full-field measurement technique.

Nowadays, the continuous improvements of the performances of digital cameras and full-field measurement techniques (e.g. DIC, grid method), have led to very accurate strain measurements with a high grade of spatial resolution and noise reduction even on small surfaces [9,10].

In this paper, the VFM is used to identify the plastic zone on a crack tip. The transition between plastic and elastic behavior can be easily obtained by FE computations but it is not possible to directly individuate it from experimental measurements of the strain field. Here it is demonstrated that the VFM can be conveniently used to this purpose. The

identification is performed starting from the strain field measured close to the crack tip. Suitable virtual fields are defined so that the contribution of the external forces is zeroed. These virtual fields are generated using piecewise functions [11], the virtual displacement on the nodes placed at the boundary of the inspected area are set to zero. An error function is then developed to assess the zones where the elastic behavior is not fulfilled. This error indicates the deviation from the linear elastic behavior, when it exceeds a threshold value, the corresponding material point is considered part of the plastic zone. It is worth noting that no force measurement is required with this approach.

The procedure is validated by means of simulated experiments. A FE model of standard CT tests is developed, then strain fields at different levels of spatial resolution are generated, synthetic noise is introduced and, eventually, the VFM is applied to evaluate the size of the plastic zone. The theoretical plastic zone obtained with the numerical model is compared with the one individuated with the proposed technique. The sensitivity of the method as well as the influence of the adopted full-field measurement technique is discussed in detail.

NUMERICAL MODEL

In this section, the FE model used to generate the simulated experiment is described. A standard CT-test according to ASTM is developed. CT-test concerns with ASTM standard testing to evaluate material toughness and it leads to appraise the residual load-carrying capacity of a cracked structure. In this test the preloaded crack specimen is held by a clevis and pin arrangement and material fracture toughness can be obtained in terms of stress intensity factor K or the J-integral. Standard compact tension (CT) test, standardize by the ASTM, involves testing of single edge notched specimen that has been fatigue pre-cracked by tension loading.
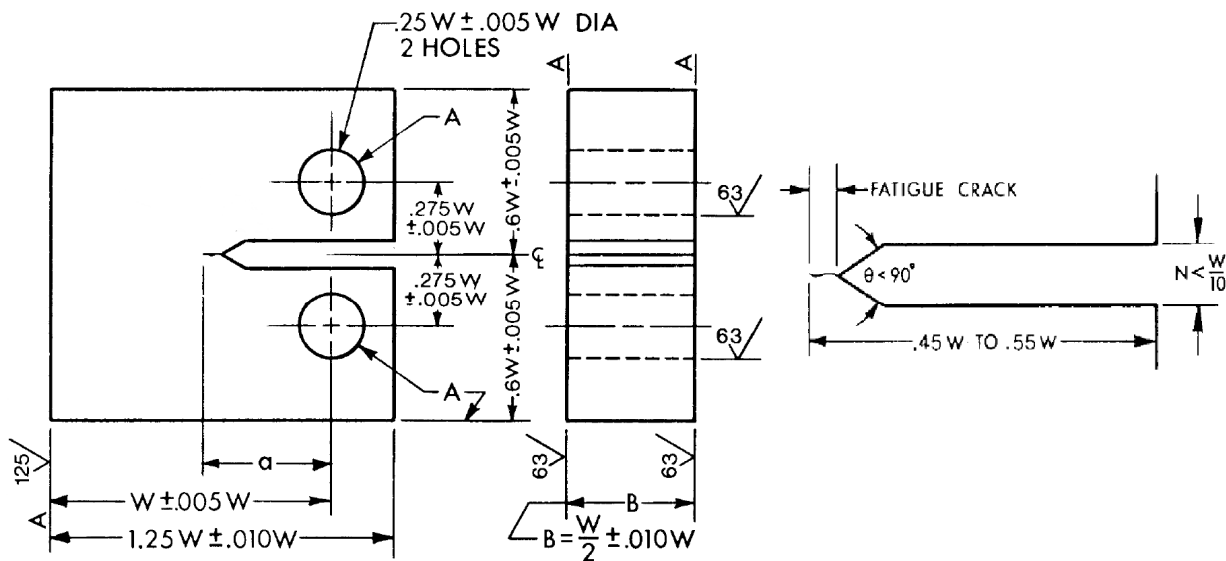

Figure 1: Compact Tension Test (CT-Test) Standard proportions and tolerances [12].

The standard specimen proportions and dimensions [12] are shown in Fig. 1, here a value of *w* = 50 mm is chosen. The minimum fatigue crack length should be considered as 0.025*w*, i.e. 1.25 mm in this case.

CT test specimen testing apparatus [13] includes pins and clevis to hold the specimen and an equal displacement or load is applied on upper and lower clevis (Fig. 2).

A steel-like material is used in the FE model of the specimen, with a Young's modulus of 210 GPa and a Poisson's ratio of 0.3. The true stress - true strain curve of the material is described by a Swift law, that is:

$$\sigma_t = K(\sigma + \varepsilon_0)^n \tag{1}$$

The values of the adopted parameters are summarized in Tab. 1. With such values, the initial yield stress of the material is 475.3 MPa, which is a rather common value for many types of steels.
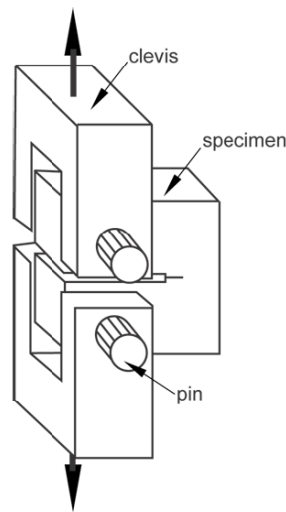
Figure 2: Compact Tension Test (CT-Test) testing apparatus [13].

E [GPa]	υ	K [MPa]	ε_0	n	σ_Y [MPa]
210	0.3	1000	0.02	0.2	457.3

Table 1: The specimen's material properties.

FE model characteristics

The specimen is modelled as three dimensional in order to keep into account the three-axial state of stress which develops close to the crack tip. The commercial FEM software Abaqus/CAE and Abaqus python scripting were used in order to have flexibility in parametric changes of model characteristics e.g. seed, mesh, crack definition, etc. In order to reduce the mesh size and computation CPU time, symmetry through thickness along the z axis (x-y plane) is considered. Rigid points at the upper and lower holes are used to reproduce the effect of pins and clevises. A fair mesh is implemented on specimen and a rectangular region with fine mesh is created along the edge crack tip to improve the crack tip singular element [14]. Domain mesh and instance section mesh are indicated in Fig. 3. Note that a rectangular section is used in order to ease the exporting nodal results to Matlab for post processing purposes.
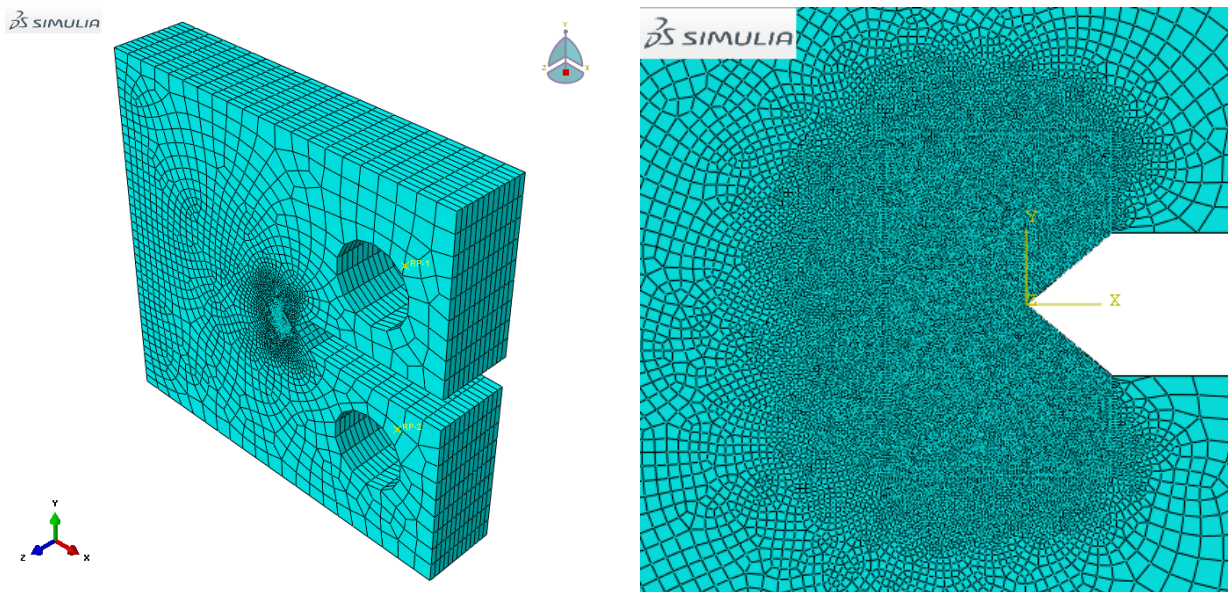

Figure 3: x-y plane symmetric specimen mesh and fine mesh at crack tip.

The specimen is loaded up to 50 KN. The crack is defined as a contour integral crack and the initial fatigue crack is assigned as crack seam. Moreover q-vector is implemented to define the crack direction. To avoid singularity at the crack tip, the mid-side node parameter moves on the element sides adjoining the collapse edge to the ¼ points of the elements which creates a $1/\sqrt{r}$ singularity in strain [14]. Therefore mid-side node parameter is set to 0.25. With the intention of avoiding negative eigenvalues and better convergence dissipated fraction energy is considered as well.

The stress intensity factor for standardized CT-test specimen can be obtained as a function of geometry and applied load as following [13]:

$$K_I = \frac{P}{Bw^{1/2}}\left[29.6\left(\frac{a}{w}\right)^{1/2} - 185.5\left(\frac{a}{w}\right)^{3/2} + 655.7\left(\frac{a}{w}\right)^{5/2} - 1017\left(\frac{a}{w}\right)^{7/2} + 639\left(\frac{a}{w}\right)^{9/2}\right] \tag{2}$$

Where P is the applied load, B and w are specimen geometry parameter and a is the crack length. The calculated stress intensity factor is compared with the one computed by Abaqus, see Tab. 2, a good agreement is found.

Analytical K_I [MPa mm$^{0.5}$]	Numerical K_I [MPa mm$^{0.5}$]
1489.071	1470.07

Table 2: Stress intensity factor comparison.

The plastic zone can be evaluated from the FE model looking at the equivalent accumulated plastic strain. In Fig. 4 the equivalent plastic strain close to the crack tip is illustrated as a contour plot. Two sections of the specimen are considered, on the left the external surface of the specimen is shown, on the right the mid-section of the specimen. The 3D FE model allows to reproduce the transition between plane stress (on the surface) and plane strain (inside the specimen). Since the strain measurement with optical methods is possible only on the external surface, this situation will be analysed in the following assuming the plane stress condition. This is necessary to estimate the stress field from the measured strain field, see next section.
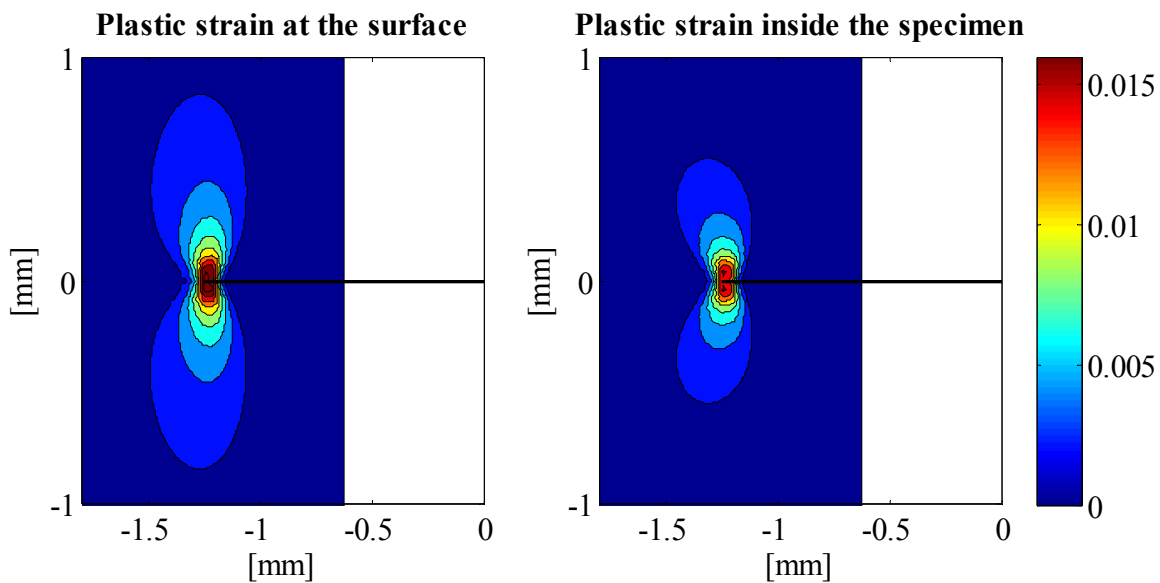

Figure 4: Plastic zone close to the crack tip on the specimen surface and in the mid-section

APPLICATION OF THE VIRTUAL FIELDS METHOD

The VFM relies on the principle of virtual works that, for a solid of any shape of volume V and surface ∂V, if there are no body forces acting on the solid, can be written as

$$\int_V \boldsymbol{\sigma} : \boldsymbol{\varepsilon}^* \, dV = \int_{\partial V} \mathbf{T} \cdot \mathbf{u}^* \, dS \tag{3}$$

where $\boldsymbol{\sigma}$ is the stress tensor, $\mathbf{T}$ is a surface force acting at the boundary and $\mathbf{u}^*$ and $\boldsymbol{\varepsilon}^*$ are a kinematically admissible virtual fields and the corresponding virtual strain fields, respectively. In case of in-plane tests with constant thickness, the problem reduces to a 2-D situation and Eq. 3 can be rewritten as:

$$t \int_S \boldsymbol{\sigma} : \boldsymbol{\varepsilon}^* \, dS = t \int_{\partial S} \mathbf{T} \cdot \mathbf{u}^* \, dl \tag{4}$$

where t is the specimen thickness. Considering an isotropic elastic material behaviour, the stress tensor can be written as a function of strain field according to the constitutive equations, for plane stress it follows:

$$\begin{pmatrix} \sigma_{xx} \\ \sigma_{yy} \\ \tau_{xy} \end{pmatrix} = \frac{E}{1-\nu^2} \begin{bmatrix} 1 & \nu & 0 \\ \nu & 1 & 0 \\ 0 & 0 & \frac{1-\nu}{2} \end{bmatrix} \begin{pmatrix} \varepsilon_{xx} \\ \varepsilon_{yy} \\ \gamma_{xy} \end{pmatrix} \tag{5}$$

with E and ν which are the Young's modulus and the Poisson's ratio, respectively. The strain field is the one measured during the experiment by a full-field optical technique. The virtual fields involved in Eq. 4 can be arbitrarily chosen provided that they are kinematically admissible [1]. They can be defined using piecewise functions as it occurs in FE models [1,11]. In this case the virtual displacement $\mathbf{u}^*$ is written as a function of the nodal coordinates $\underline{\mathbf{u}}^{(e)}$ of an element. according to the element shape functions $\mathbf{N}$:

$$\mathbf{u}^* = \mathbf{N}\mathbf{u}^{(e)} \tag{6}$$

The strain can be obtained as well from the nodal coordinates as:

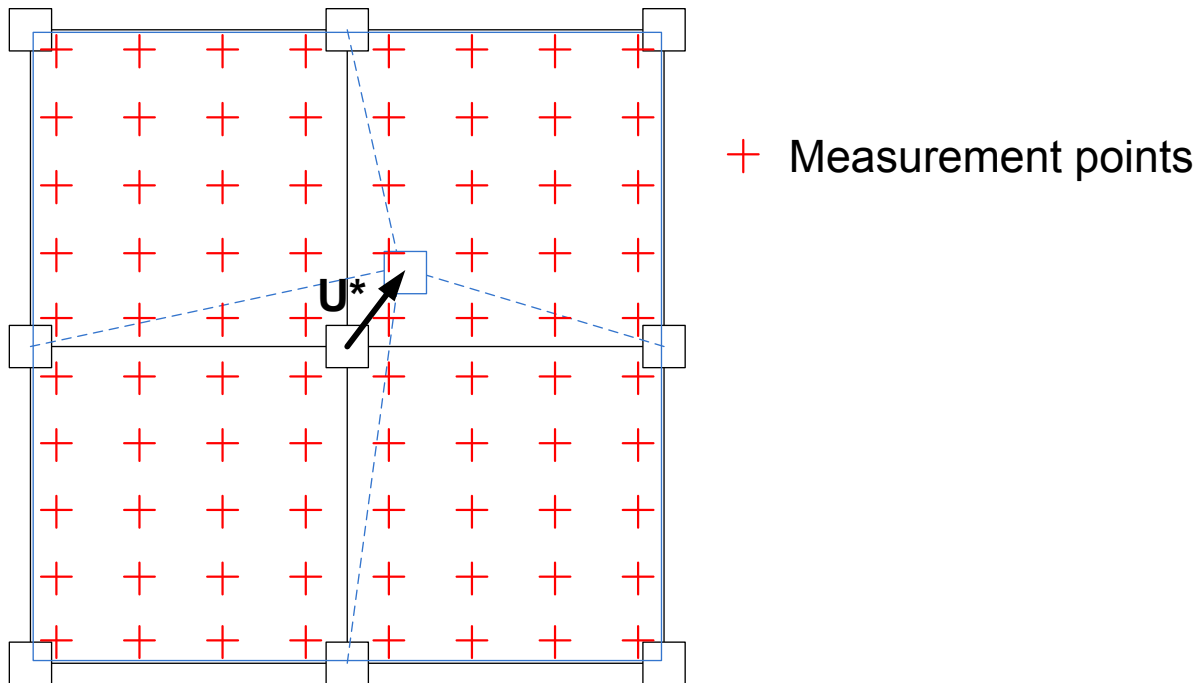$$\boldsymbol{\varepsilon}^* = \mathbf{B}\mathbf{u}^{(e)} \tag{7}$$

Figure 5: Virtual fields definition: the virtual fields are defined using 4 elements with the external nodes fixed and the internal one moved of a virtual displacement $\mathbf{U}^*$. The area includes a certain number of measurement points

In the present case four elements were used, as illustrated in Fig. 5. The 8 nodes at the boundary are kept fixed while the internal node is moved. In such a way the virtual displacement at the boundary is equal to zero and the second term of Eq. 4 vanishes. This means that if the material has a linear elastic behaviour, the first term is identically null in each zone of the specimen. Close to the crack tip, however, the material behaviour deviates from elasticity because plastic deformation locally occurs. In this case, Eq. 4 is not valid anymore, this discrepancy can be considered as an indication of the plasticity occurrence. With this assumption, an error function *Err* can be defined

$$Err = \frac{1}{N_v} \sum_{i}^{N_v} \frac{1}{S} \left| \int_S \boldsymbol{\sigma} : \boldsymbol{\varepsilon}_i^* \, dS \right| \qquad (8)$$

where N_v is the number of independent virtual fields employed. The unit of this error is a specific energy. The larger the error function the most likely the inspected zone undergoes plastic deformation. The error is normalized on the surface area S so that its value is not influenced by its size. Indeed, the area can be varied in order to include more or less measurement points. It is worth underlying that no other assumptions are made on the plasticity law, i.e. the identification of the plasticity material properties are not necessary to detect the plastic zone.

The area of the virtual field is moved along the measured strain field as a sort of "probe" which detects the likelihood of plastic deformation occurrence inside the area. In such a way it is possible to define an error map close to the crack tip. At this point, an error threshold is defined and the plastic zone is defined as the area where the threshold is overtaken. In this paper the value of the threshold was set empirically, as it will be shown later on. This simplification is justified since this paper aims to describe the method and its potentiality. An in depth study is required in future works to evaluate a proper way of setting this threshold.

RESULTS AND DISCUSSION

As first step, the FEM results have to be reshaped to simulate an experimental full-field measurement. A field of view of around 2 × 2 mm close to the crack tip is chosen. This area is quite small but can be framed using suitable optics [10]. Along this surface, the strain field can be measured using a full-field optical technique as, for instance, the grid method or the DIC. According to the used technique and the experimental conditions, (size of the grid or the speckle pattern, light conditions, etc.) the spatial resolution can vary. In this study, three different spatial resolutions are used 0.1, 0.05 and 0.01 mm. The first one can be obtained quite easily using the grid method [15], while the last ones are more challenging to obtain in a real experiment. The strain field obtained with the FEM is reshaped on a regular grid with the assigned spatial resolution using interpolation functions, i.e. the "griddata" Matlab function. The results are shown in Fig. 6. The influence of the spatial resolution is highlighted, a spatial resolution of 0.1 mm allows a rather coarse description of the strain fields. In this particular application the spatial resolution is critical because of the large strain gradient encountered close to the crack tip.

In order to reproduce an actual test, the experimental noise was simulated as a random Gaussian distibution applied directly to the strain fields. Two level of noise were used, with a standard deviation of $5 \cdot 10^{-4}$ and $2 \cdot 10^{-3}$ m/m. The first reproduce a moderate noise level, the second a severe one. The obtained strain fields are illustrated in Fig. 7. The same spatial resolution of 0.05 mm is used.

At this point the VFM was applied to evaluate the plastic zone. As first test, the strain field was evaluated using a spatial resolution of 0.01 mm. In this case the field of view has 201×201 measurement points. The VFM was defined over an area of 40×40 measurement points. 24 independent virtual fields were used in Eq. 8 by varying the displacement $\mathbf{U}^*$ of the central node as follows:

$$\mathbf{U}^* = \left| \mathbf{U}^* \right| \{ \cos \vartheta, \sin \theta \} \quad \text{with} \quad \vartheta = [0 : \pi / 12 : 2\pi[\qquad (9)$$

The results are illustrated in Fig. 8. Two thresholds were used, the blue line represents a threshold of 5 J/mm³ and the purple line a threshold of 10 J/mm³. These value are empirically chosen. In the same graph, the theoretical plastic zone from FEM is shown. The proposed method can detect a level of plastic strain of around 1% and it is not influenced by the noise level. However, a mismatch respect to the shape of the plastic zone is observed. This effect can be due to the size of the VFM area which includes around 40 measurement points. Moreover the used virtual fields are very simple, involving only 4 elements, in the future more effective virtual fields should be individuated.
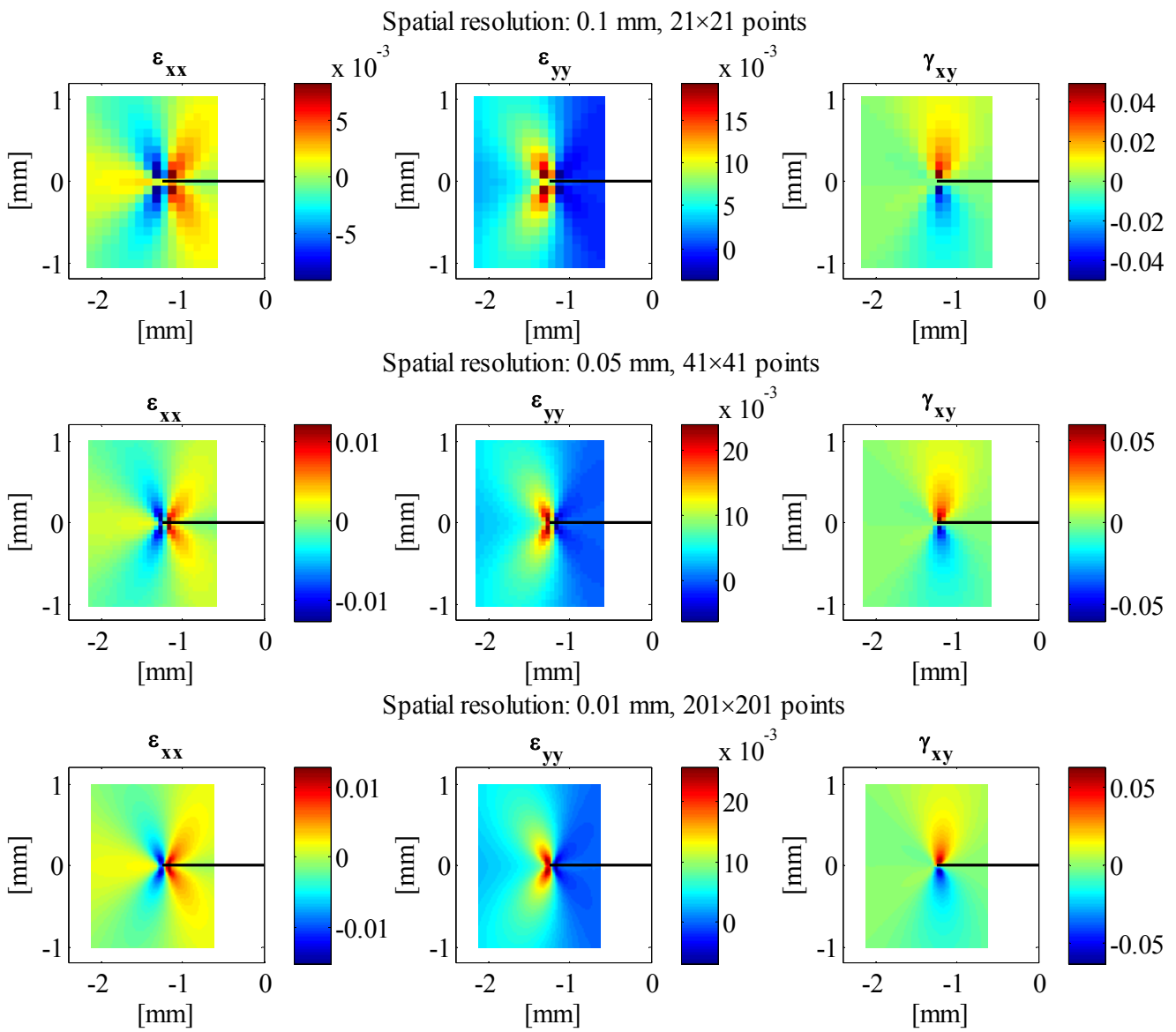
Figure 6: Strain field at the crack tip using different values for the spatial resolution.
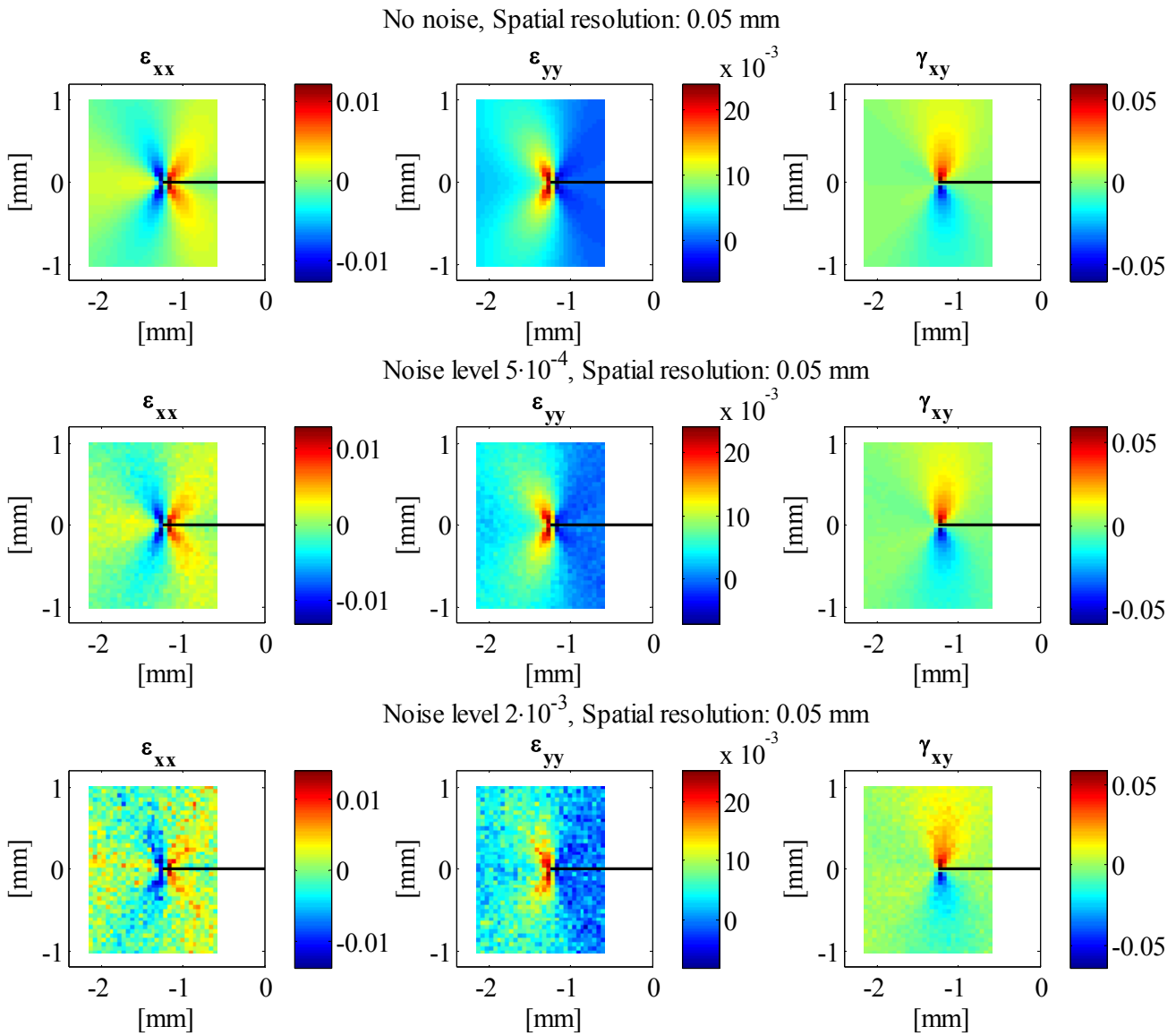
No noise, Spatial resolution: 0.05 mm

Noise level $5 \cdot 10^{-4}$, Spatial resolution: 0.05 mm

Noise level $2 \cdot 10^{-3}$, Spatial resolution: 0.05 mm

Figure 7: Strain field at the crack tip using different noise level.

No noise   **Noise level $5 \cdot 10^{-4}$,**   **Noise level $2 \cdot 10^{-3}$,**
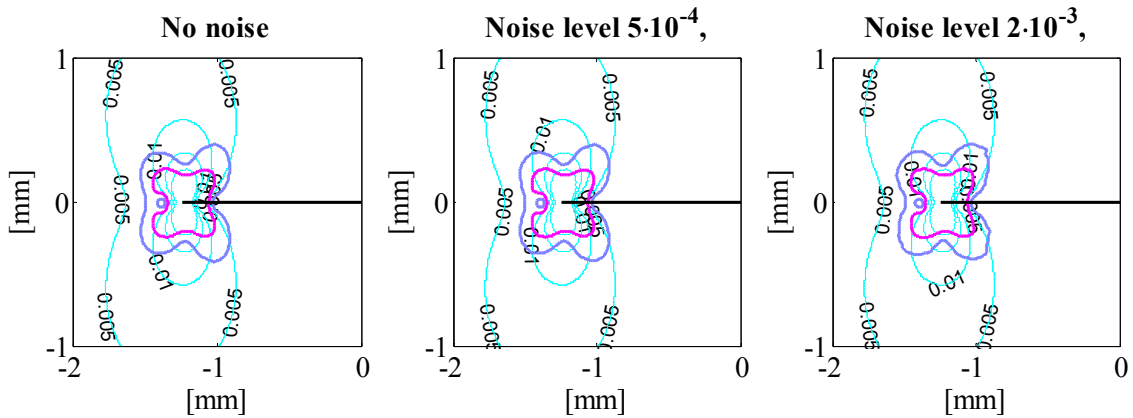
Figure 8: Identification of the plastic zone at different level of noise using a spatial resolution of 0.01 mm. The VFM is applied on a 0.4 mm area which includes 40×40 measurement points.

A second test was conducted using a lower spatial resolution, namely 0.1 mm. The same VFM area is used so that, in this case only 4×4 measurement points are included. Nonetheless, when a small amount of noise is used, the results are still stable. At the higher level of noise, using the lower threshold of 5 J/mm^3, the plastic area is remarkably affected by the noise. However a stable result is obtained if a threshold of 10 J/mm^3 is used. The shape is similar to the one obtained at the higher spatial resolution.
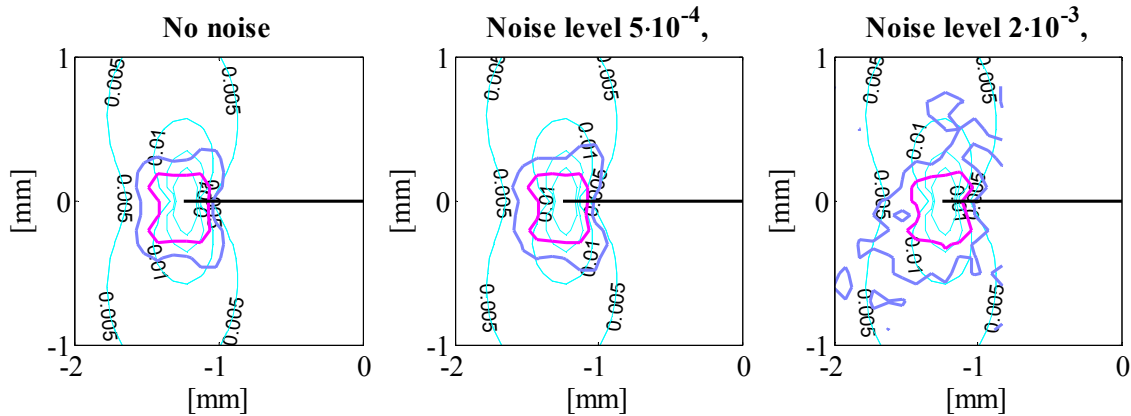

Figure 9: Identification of the plastic zone at different level of noise using a spatial resolution of 0.1 mm. The VFM is applied on a 0.4 mm area which includes 4×4 measurement points.

The procedure shows good potentiality to be applied also with noisy measurement at low spatial resolution. However the difference in shape should be analysed in more details to assess the reliability of the proposed method.

CONCLUSIONS

The VFM was used to identify the plastic zone close to the crack tip in a CT-test. The procedure was demonstrated by means of simulated experiments. A complete 3D FE model was developed to realistically reproduce the test. Then the measured strain fields were simulated by interpolating the FE nodal results. The nodal strain fields were reshaped according to a regular grid the reproduces the field of view of the measurement. The spacing between the measurement points is defined according to the spatial resolution that has to be simulated. The application of the VFM produced the following outcomes:

- the procedure allows to individuate the plastic zone with no assumption on the yielding stress and the plastic behaviour of the material;
- the procedure is stable and can be used also with low spatial resolution and noisy measurements;
- a mismatch is obtained between the shape of the identified plastic zone and the shape of accumulated plastic strain obtained in the numerical model.

The used virtual fields should be enhanced to improve the shape detection of the plastic zone. The definition of the error threshold should be chosen using a less empirical criterion, for instance coupling the error level with the noise level of the measurements. This aspects will be treated in future studies.

REFERENCES

[1] F. Pierron, M. Grédiac, The Virtual Fields Method, Springer, (2012).
[2] M. Rossi, F. Pierron, Comput. Mech., 49 (2012) 53.
[3] M. Grédiac, F. Pierron, Int. J. Plasticity, 22 (2006) 602.
[4] G. Palmieri, M. Sasso, G. Chiappini, D. Amodio, Strain, 47 (2011) 196.

[5] T. Guélon, E. Toussaint, J.-B. Le Cam, N. Promma, M. Grédiac, Polymer Testing, 28 (2009) 715.

[6] F. Pierron, P. Forquin, Strain, 48 (2012) 388.

[7] A. Giraudeau, F.Pierron, J. Sound. Vib., 284 (2005) 757.

[8] S. Avril, M. Bonnet, A. S. Bretelle, M. Grédiac, F. Hild, P. Ienny, F. Latourte, D. Lemosse, S. Pagano, E. Pagnacco, F. Pierron, Exp. Mech., 48 (2008) 381.

[9] M. Bornert, F. Brémand, P. Doumalin, J.-C. Dupré, M. Fazzini, M. Grédiac, F. Hild, S. Mistou, J. Molimard, J.-J. Orteu, L. Robert, Y. Surrel, P. Vacher, B. Wattrisse, Exp. Mech., 49 (2009) 353.

[10] R. Moulart, R. Rotinat, F. Pierron, G. Lerondel, Opt. Laser. Eng., 45 (2007) 1131.

[11] S. Avril, M. Grédiac, F. Pierron, Comput. Mech., 34 (2004) 439.

[12] ASTM Standards, Standard Test Method for Plane-Strain Fracture Toughness of Metallic Materials, ASTM E399- 90, American Society for Testing and Materials, Philadelphia, (1997).

[13] T. L. Anderson, Fracture Mechanics: Fundamentals and Applications, CRC Press, (1991).

[14] M. Denda, Y.F. Dong, Engineering Analysis with Boundary Elements, 23 (1999) 35.

[15] M. Rossi, F., Pierron, Int. J. Solids Struct., 49 (2012) 420.